PERGAMON

International Journal of Heat and Mass Transfer 43 (2000) 1975–1985

International Journal of HEAT and MASS TRANSFER

www.elsevier.com/locate/ijhmt

Slot jet impingement heat transfer from circular cylinders

C.S. McDaniel, B.W. Webb*

Mechanical Engineering Department, 435 CTB, Brigham Young University, Provo, UT 84602-4102, USA

Received 10 December 1998; received in revised form 17 August 1999

Abstract

The heat transfer characteristics of circular cylinders exposed to slot jet impingement of air has been studied experimentally. The study focused on Reynolds numbers (based on nozzle average exit velocity and cylinder diameter) in the range 600–8000. Both contoured orifice and sharp-edged orifice jet configurations were investigated for cylinder diameter-to-jet width spacings of 0.66, 1.0 and 2.0, and for jet exit-to-nozzle width spacings in the range $1 < z/w < 11$. Reference measurements were made with the same cylinder in infinite parallel flow in a wind tunnel. The results reveal that the slot jet yields considerably higher average heat transfer from the cylinder when compared to the infinite parallel flow case on the basis of identical average velocity in the slot jet and infinite flow configurations. As with slot jet impingement heat transfer from flat surfaces, there appears to be a nozzle-to-cylinder spacing, scaled by nozzle width, which exhibits a maximum in heat transfer. The average heat transfer characteristics of the cylinder are correlated empirically.

1. Introduction

Jet impingement heat transfer is used in a broad spectrum of industrial applications including drying of textiles and paper, a variety of manufacturing processes, annealing of metals and glass, thermal control of electronics, etc. Past reviews of the related literature details both fundamental characterization studies and applications [1–4]. One segment of the research which deals with slot jet impingement heat transfer from cylinders has received only limited attention. Schuh and Persson [5] characterized the heat transfer from circular cylinders cooled by contoured orifice slot jets in the Reynolds number range 20,000–50,000. Kumada et al. [6] investigated the local mass transfer from such a cylinder for Reynolds numbers ranging from 43,000 to 200,000 using a contoured orifice. The Sherwood number was found to depend on Reynolds number according to the relation $\overline{Sh} \sim Re^m$ where m was found to vary between 0.6 and 0.68 depending on nozzle width. Sparrow and Alhomoud [7] employed a sharp-edged orifice jet in a similar study with and without cylinder offset for Reynolds numbers between 5000 and 60,000. The average Nusselt number was found to vary as $\overline{Nu} \sim Re^{3/4}$ for $Re > 20{,}000$. The $\overline{Nu} \sim Re$ relationship was observed to be different at lower Reynolds number, but the dependence was not characterized.

While many industrial applications may fall in the Reynolds number range previously investigated for this configuration, a number of uses of the cooling technique feature low velocities and/or small cylinder diameters, and would therefore fall naturally in the lower Reynolds number range. Additionally, while jet impingement has been investigated in independent studies for jets issuing from both contoured and sharp-edged orifices, little has been done to correlate and

* Corresponding author. Tel.: +1-801-378-6543; fax: +1-801-378-5037.

E-mail address: webb@byu.edu (B.W. Webb).

0017-9310/00/$ - see front matter
PII: S0017-9310(99)00267-7

Nomenclature

A_s	cylinder surface area
d	cylinder diameter
$\bar{h}$	average heat transfer coefficient
k	thermal conductivity
$\overline{Nu}$	average Nusselt number, $\bar{h}d/k$
$\overline{Nu}_\infty$	average Nusselt number for cylinder in infinite parallel flow
q	power dissipation in cylinder
Re	Reynolds number based on cylinder diameter, Vd/v
T_j	jet temperature
T_c	average cylinder temperature
V	average jet exit velocity
w	nozzle width, Fig. 1
z	distance between nozzle exit and cylinder forward stagnation point, Fig. 1
v	kinematic viscosity

compare data from these nozzle types. The research reported here seeks to fill this gap by characterizing slot jet impingement cooling of circular cylinders in the Reynolds number range 600–8000 for both contoured and sharp-edged orifices. Three different slot widths were investigated for a range of nozzle-to-cylinder spacings. Experimental data for infinite parallel flow cooling of cylinders were also collected to serve as benchmark against which heat transfer for the slot jet configuration could be compared. Finally, the data are correlated empirically for use in thermal design situations.

2. Experimental apparatus and procedure

The apparatus for study of heat transfer from a circular cylinder exposed to impingement slot jet flow included the flow metering and jet generation apparatus, heated cylinder, and instrumentation. These will now be described in detail, followed by a brief description of the experimental procedure and uncertainty in the data.

2.1. Metered flow and jet nozzles

The jet was generated by directing supply air flow through flow meters, into a baffled plenum, and subsequently through the nozzle for impingement on the heated cylinder, as shown schematically in Fig. 1. A regenerative blower powered by a variable speed DC motor was used to develop the necessary air supply pressure and flow. The air flow rate was metered by passing through a combination of three bypass flowmeters connected in parallel, such that the total flow rate is the sum of the flow rates through the three flowmeters (see Fig. 1) The three flowmeters each feature a different measurement range in order to optimize the accuracy. The total flow capacity of the system was limited to 0.026 m^3/s (55 CFM). The uncertainty in measured flow rate was 5% for all flowmeters.

The metered air flow was directed to a plenum with baffle plate, used to decelerate the flow from the plenum supply inlet (Fig. 1). Maximum velocities in the plenum were calculated to be approximately 0.5 m/s. The plenum and flow baffle were designed to provide near-unidirectional flow to the nozzle. The plenum chamber was 40 cm high, 32 cm wide, with the same depth (normal to the figure) as the length of the heated cylinder, 15.2 cm.

Two types of nozzles were used in the experiments, as shown in Fig. 1. A contoured nozzle with contour radius of 2.54 cm was constructed of shaped balsa wood and covered with Mylar sheeting to provide smooth walls. A sharp-edged orifice was built from 0.5 cm thick Plexiglas which was cut back at a 45° angle on the flow exit side. Both nozzles were built in two sections permitting them to be positioned at different orifice exit widths w.

Positioning arms were attached to the walls of the

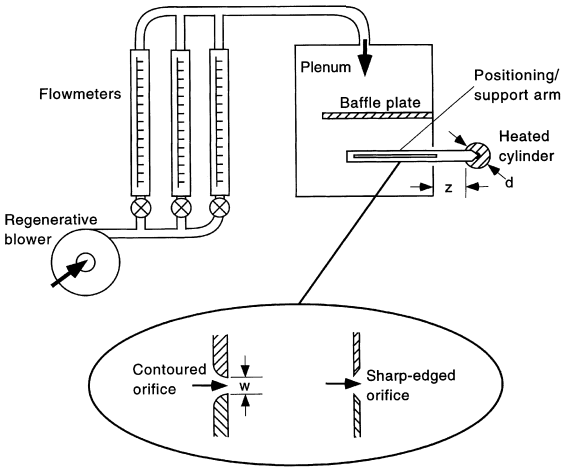

Fig. 1. Schematic illustration of flow metering and jet generation assembly.

plenum chamber to which the heated cylinder was suspended, as shown in Figs. 1 and 2. A slot in the positioning arms permitted the cylinder to be moved relative to the nozzle exit, allowing study of the heat transfer behavior over a range of nozzle-to-cylinder spacing z.

2.2. Heated cylinder

The heated cylinder was constructed from oxygen-free copper rod of diameter $d = 1.27$ cm, and length 15.2 cm. A 0.24 cm-diameter hole was bored through the center of the rod its entire length. Epoxy-coated nichrome wire was drawn through the center hole, and the remaining space was filled with epoxy, as shown schematically in Fig. 2. The nichrome heating wire was connected to larger gage electrical supply wire as close to the cylinder as possible. The electrical supply wire was then connected to a precision DC power supply which provided the electrical power for ohmic heating. The current drawn by the nichrome wire during heating was given by the power supply digital readout to within ± 0.01 A. Small-gage wire was attached to the nichrome wire at the same location where power supply leads were attached, and voltage was read with a digital voltmeter with ± 0.01 V accuracy. The total power dissipation was then calculated as the product of the measured current and voltage. In determining the heating rate for the cylinder, the total power dissipation was reduced by the small length (< 0.3 cm) of nichrome wire which protruded from each end of the cylinder, and which was ohmically heated outside of the copper cylinder. The power dissipation in the protruding length of heater wire amounted to less than 4% of the total, but a correction was made nevertheless.

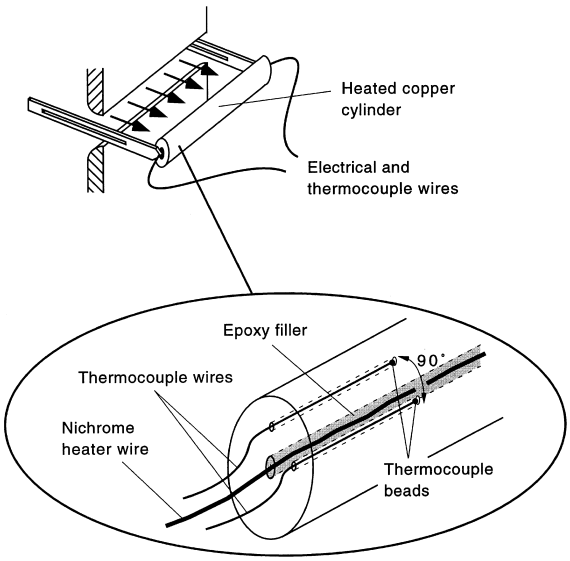

Fig. 2. Schematic illustration of heated cylinder and instrumentation.

As shown in Fig. 2, four 0.15-cm-diameter holes were drilled along the axis of the copper cylinder, two in each end, to permit temperature characterization of the cylinder. The holes were separated by 90° rotations in order to evaluate any temperature gradients around the circumference of the cylinder. The thermocouple holes were positioned radially halfway between the radius of the center hole accommodating the heater wire and the cylinder's outer surface. On one end of the cylinder both holes were drilled to a depth of 3.8 cm from the cylinder end, while at the other end holes were drilled to depths of 2.5 cm and 3.8 cm. Type K thermocouples were inserted into the holes and connected to a temperature data acquisition system capable of resolving temperature to within 0.1°C. A thermocouple was also placed inside the plenum upstream of the nozzle exit for measuring the jet exit temperature T_j. The intent in designing the heated cylinder was to place thermocouples at its spanwise center, but drilling such small-diameter access holes to this desired depth was not possible. The final hole placement was a fabrication compromise which permitted evaluation of temperature gradients both along the cylinder length and around its periphery. The Biot number for the cylinder (based on measured average heat transfer coefficients) indicated that the cylinder was isothermal; the maximum Biot number was 0.005. The isothermal nature of the cylinder was borne out by the cylinder temperature measurements. The maximum temperature variation in the cylinder in all experiments was less than 5% of the difference between the average cylinder and jet temperature, $(T_c - T_j)$. The variation was more typically 3% or less.

The outer surface of the pure copper cylinder was repeatedly polished with successively finer polishing powder to a mirror finish to minimize the radiation transfer. Given the composition of the cylinder and the finish achieved during polishing, the emissivity was estimated to be less than 0.05. Correction to the total power dissipated from the cylinder was made for the radiation transfer, which amounted to less than 4% of the total.

In order to provide benchmark heat transfer data for the case of the cylinder in infinite parallel flow, the heated cylinder was modified for use in a low-speed, low-turbulence wind tunnel. The tunnel featured a test section of cross-sectional area 36 × 36 cm, and was operated in suction mode. Smooth plastic cylinders of the same outer diameter as the heated copper cylinder were attached to each end of the heater. The entire assembly was then suspended such that the heated cylinder was positioned in the center of the wind tun-

nel. The thermocouple and nichrome heater supply wires were drawn through the plastic support cylinders, and out of the wind tunnel through mating holes in the walls. The wind tunnel velocity was measured using a 0.24 cm diameter pitot tube. Stagnation-static pressure differences were measured using a precision inclined manometer. The wind tunnel speed was controlled, providing capability to measure the infinite parallel flow heat transfer from the heated cylinder to a minimum Reynolds number (based on wind tunnel freestream velocity and cylinder diameter) of 2500. Below this, the wind tunnel operation was unsteady and unsuitable for testing. The wind tunnel measurements permitted confirmation of the accepted cylinder-in-crossflow correlation of Churchill and Bernstein [8]:

$$\overline{Nu}_\infty = 0.3 + \frac{0.62 Re^{1/2} Pr^{1/3}}{[1+(0.4/Pr)^{2/3}]^{1/4}} \times \left[1 + \left(\frac{Re}{282,000}\right)^{5/8}\right]^{4/5} \quad (1)$$

The correlation was then used as the basis for evaluating enhancement of heat transfer from the slot jet impingement configuration over the full range of Reynolds numbers studied here.

The average heat transfer coefficient was calculated from known power dissipated q (corrected for radiation), cylinder surface area A_s, and measured temperatures as

$$\bar{h} = q/A_s(T_c - T_j) \quad (2)$$

where T_c is the average of the four temperatures measured within the heated cylinder. The average Nusselt number was then determined as

$$\overline{Nu} = \bar{h}d/k \quad (3)$$

As with the infinite correlation of Churchill and Bernstein [8], the thermophysical properties were evaluated at the film temperature, $(T_c + T_j)/2$.

Data were taken for the slot jet configuration using nozzle widths of 0.5, 1.0, and 1.5 cylinder diameters. At each nozzle width, heat transfer behavior was investigated over a range of nozzle-to-cylinder spacing z. Heat transfer data were collected for both the contoured and sharp-edged orifices. Data collected at identical experimental conditions for several tests revealed data repeatability to 3% of Nusselt number. Experimental uncertainty using the method of Beckwith et al. [9] revealed a maximum uncertainty in Reynolds number and average Nusselt number of 7% and 5%, respectively. The same holds of the wind tunnel tests.

There are three geometric parameters which describe each experimental configuration. They are the heated cylinder diameter d, the nozzle width w, and the nozzle-to-cylinder spacing z. Normalizing using the nozzle width as has been done previously [5–7] yields a range of nozzle-to-cylinder spacing of $1 < z/w < 11$ for $d/w = 0.66$, 1.0, and 2.0. The Reynolds number in this study is based on the average jet exit velocity (determined from the orifice cross-sectional area and the metered total air flow rate) and the cylinder diameter, $Re = Vd/\nu$. Note that the Reynolds number is based on cylinder diameter rather than nozzle width, (i) to provide consistency with previous data, and (ii) to allow comparison with the limiting case of heat transfer from a cylinder in infinite parallel flow The infinite parallel flow experiments were characterized also by a Reynolds number based on cylinder diameter, but with freestream velocity V. The comparison between slot jet and infinite parallel flow heat transfer is then made on the basis of slot jet exit velocity identical to the infinite flow freestream velocity.

3. Results and discussion

The dependence of the average Nusselt number on Reynolds number is shown in Figs. 3 and 4 for the three nozzle widths (cylinder diameter-to-nozzle width ratios) studied at the corresponding nozzle-to-cylinder spacings for the contoured and sharp-edged orifices, respectively. Note that for the non-dimensionalization used here and in previous studies, the dimensionless parameters d/w and z/w may not vary independently with a test matrix varying w. The data of Figs. 3 and 4 were taken with the cylinder maintained a given physical distance z from the nozzle exit at the three nozzle widths studied. Also shown in Figs. 3 and 4 are the infinite parallel flow data taken in the wind tunnel, and the corresponding cylinder-in-crossflow correlation of Churchill and Bernstein [8], given by Eq. (1). It may first be noted that the infinite flow data taken here match well the accepted correlation in the Reynolds number range studied. The maximum and average difference between experimental data and correlation are 7.6% and 3.0%, respectively. Given the good agreement between the infinite flow heat transfer data taken as part of this study and the accepted correlation, the slot jet impingement data may be compared with the infinite flow correlation, Eq. (1), to determine the degree of heat transfer enhancement.

As a free jet exits the nozzle from which it issues into a stagnant fluid environment, a potential core is formed inside which the jet centerline velocity remains at approximately the exit value. The shear layer at the boundaries between the potential core and the stagnant ambient fluid is a region of high velocity gradient and corresponding high turbulence. As the jet proceeds

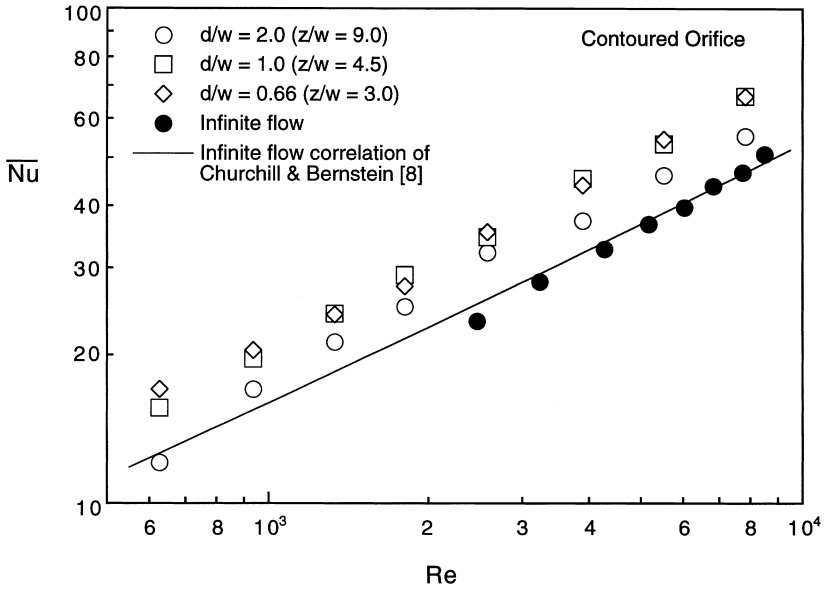

Fig. 3. Variation of average Nusselt number with Reynolds number for the contoured orifice, and comparison with infinite parallel flow data and correlation [8].

downstream the shear layer thickens until the potential core vanishes. Beyond this point the jet centerline velocity decreases monotonically. Previous data have shown the potential core for slot jets to be approximately three to eight slot widths in length. The presentation of different values of d/w with corresponding z/w as is done in Figs. 3 and 4 is a comparison of heat transfer for a given size cylinder placed a fixed distance from the nozzle exit (and along the jet centerline) for several different nozzle widths. It might be said, then, that the cylinder lies at different locations within the free jet's potential core. For jets issuing from both the contoured and sharp-edged orifice, the average Nusselt number is lowest for the $z/w = 9$ nozzle-to-cylinder

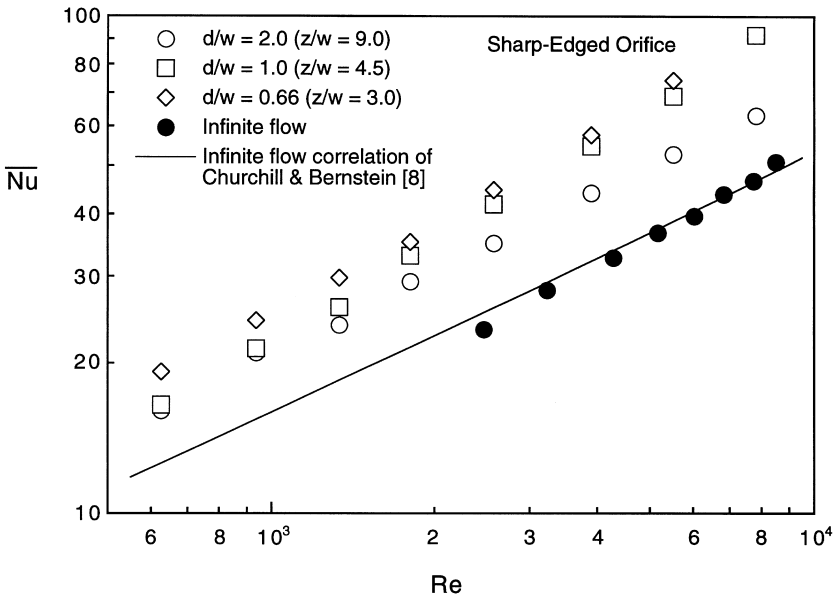

Fig. 4. Variation of average Nusselt number with Reynolds number for the sharp-edged orifice, and comparison with infinite parallel flow data and correlation [8].

spacing; the $z/w = 3.0$ and 4.5 data are considerably higher. Although not clearly evident here, there is a maximum in the $\overline{Nu} \sim z/w$ relationship which will be explored later.

Several additional general observations may be made relative to the data of Figs. 3 and 4. It appears that the average Nusselt number follows a $\overline{Nu} \sim Re^m$ relationship. The empirical constants for this relationship will be presented later. It may also be noted that slot jet impingement heat transfer from cylinders is substantially higher than the infinite parallel flow case given by Eq. (1) for the same Reynolds number (identical slot jet exit and freestream velocities). Further, the average Nusselt number data for the sharp-edged orifice is higher than the contoured orifice. All of these observations will be quantified in sections to follow.

The Nusselt number dependence on Reynolds number is shown in Fig. 5 for the contoured orifice at two different nozzle-to-cylinder physical spacings z. Unlike the data presentation of Figs. 3 and 4 where the cylinder was stationary while the jet width was increased, the cylinder in Fig. 5 is positioned at nearly the same *dimensionless* location ($z/w = 1.5$ and 1.66) for two different values of w. In other words, the cylinder's location relative to the jet potential core is nominally the same, assuming that the free jet scales with orifice width w. The figure reveals that the average Nusselt number is nearly identical for the same Re and z/w, suggesting that the dimensionless parameters used are appropriate for scaling the data. The enhancement of the slot jet impingement configuration relative to the infinite parallel flow case is again noted.

The cylinder heat transfer for slot jet impingement relative to that for cylinders in infinite parallel flow may be compared by calculating the ratio of the average Nusselt numbers for the two configurations, $\overline{Nu}/\overline{Nu}_\infty$. The value of $\overline{Nu}_\infty$ was determined from the empirical correlation of Churchill and Bernstein [8], Eq. (1), at the same velocity V. The variation of enhancement ratio with Reynolds number is shown in Fig. 6 for the two orifice configurations studied, and for a range of z/w at $d/w = 1$. It is seen that the enhancement ratio is nearly independent of Re for the contoured orifice over the range of Reynolds number studied. At the highest Reynolds number studied there is between 28 and 45% enhancement in heat transfer for the contoured slot jet over the infinite flow case. Typical magnitudes of the heat transfer enhancement for the contoured orifice of $\overline{Nu}/\overline{Nu}_\infty \approx 1.2$ are consistent with previous studies at Reynolds numbers two orders of magnitude higher than those reported here [5,6].

The sharp-edged orifice exhibits qualitative and quantitative heat transfer enhancement ratio behavior quite different from the contoured orifice for the same nozzle width ($d/w = 1$). While $\overline{Nu}/\overline{Nu}_\infty$ for the contoured orifice is relatively independent of Re, the enhancement for the sharp-edged orifice increases markedly with Reynolds number (see Fig. 6). Indeed, the enhancement near $Re = 8000$ for the sharp-edged orifice is nearly 100% over the infinite flow value. It may be speculated that the enhancement would exhibit a maximum or asymptote with Reynolds number, although such could not be confirmed with the regenerative blower employed due to limited capacity. It is quite clear that the sharp-edged orifice yields signifi-

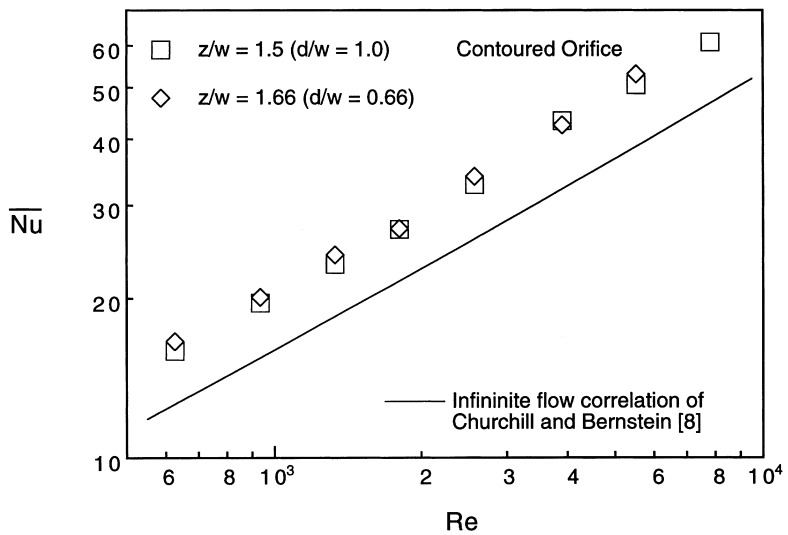

Fig. 5. Comparison of average Nusselt number with Reynolds number for the same nominal dimensionless nozzle-to-cylinder spacing z/w.

cantly better heat transfer characteristics than the contoured orifice, all other experimental conditions remaining the same.

Schuh and Persson [5] suggest that the heat transfer enhancement over that found in classical infinite parallel flow is due to increased turbulence in the slot jet configuration. The higher turbulence provides greater energy for the flow to remain attached to the cylinder as it proceeds around the cylinder surface from the forward stagnation point. Of course, the two slot configurations yield markedly different mean flow characteristics as well. The differences in magnitude and Reynolds number dependence between the two orifices studied may be explained in terms of the free jet flow structure generated by each. The flow through the contoured orifice tends to remain attached to the surfaces of the nozzle until it is discharged at the nozzle exit, and produces a nearly uniform velocity profile. By contrast, the flow through the sharp-edged orifice experiences separation at the nozzle exit and a vena contracta. The resulting velocity profile is non-uniform with centerline velocity higher than that at the nozzle edges [1,10]. Higher velocity gradients in the velocity profile also yield greater shear and resulting higher levels of turbulence. The cylinder exposed to flow from the sharp-edged orifice thus experiences higher velocity fluid at its front face. Further, the vena contracta effect is enhanced at higher Reynolds numbers. Therefore, the enhancement ratio increases at increasing Reynolds number.

Although not shown in Fig. 6, values of the ratio $\overline{Nu}/\overline{Nu}_\infty$ less than unity (approximately 0.95) were found for the contoured orifice at the lowest Reynolds number studied, and for extremes in the nozzle-to-cylinder spacing (low and high z/w). In the case of very small z/w the flow is deflected away from the front surface of the cylinder and lacks energy to re-attach on the backside at these low Reynolds numbers. The backside of the heated cylinder thus experiences relatively ineffective cooling flow. At extreme large z/w the cylinder is located beyond the free jet's potential core and the jet centerline velocity is reduced by the stagnant ambient fluid; the approaching free jet momentum is degraded to a level where the high turbulence cannot compensate for reduced impingement velocity.

Fig. 7 shows $\overline{Nu}$ vs z/w data for the contoured orifice at $d/w = 2.0$ for all Reynolds numbers studied. The figure reveals that a maximum in $\overline{Nu}$ occurs at a nozzle-to-cylinder spacing between 3 and 7 nozzle widths. This spacing corresponds to the end of the jet potential core [1–3]. The maximum is more evident at higher Reynolds numbers, where the effect of shear-induced turbulence at the tip of the jet's potential core is more pronounced. In the most extreme case ($Re = 7820$) the peak Nusselt number is roughly 20% higher than the minimum Nusselt number. Such maxima were also observed with other nozzle widths, and for both orifice configurations. It should not be surprising that this same phenomenon observed for jet impingement on flat surfaces also occurs with impingement cooling of cylinders.

The maximum in Nusselt number for z/w between 3 and 7 is also evident in the ratio $\overline{Nu}/\overline{Nu}_\infty$, and reveals

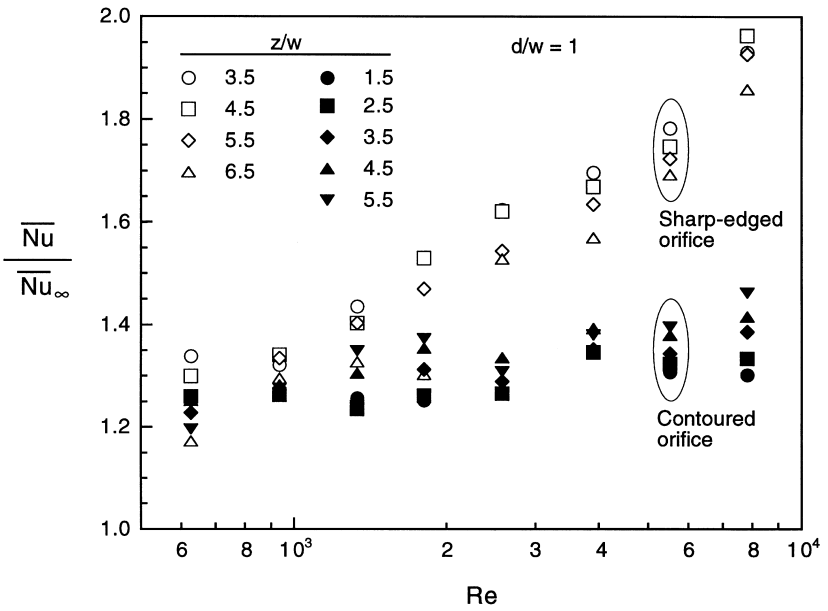

Fig. 6. Variation of heat transfer enhancement factor $\overline{Nu}/\overline{Nu}_\infty$ with Reynolds number for the two orifices studied at $d/w = 1.0$.

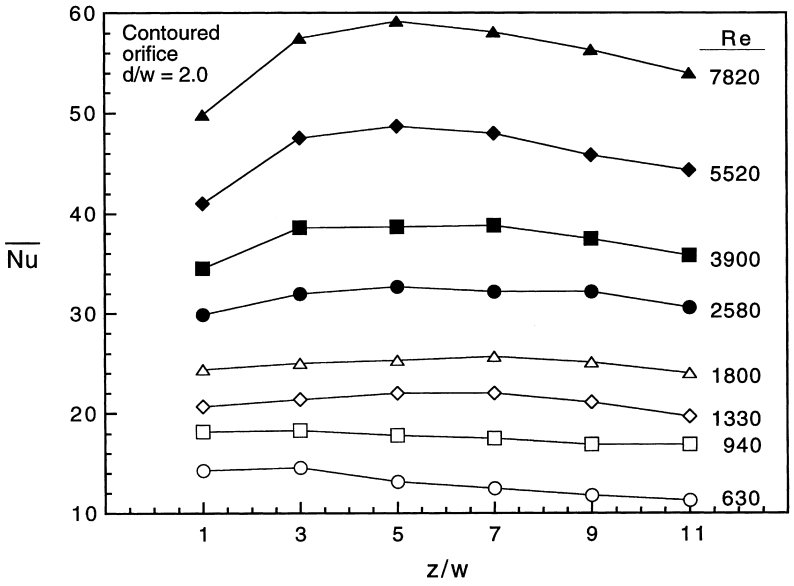

Fig. 7. Variation of average Nusselt number with z/w for the contoured orifice, $d/w = 2.0$.

the magnitude of the heat transfer enhancement due to the formation of a potential core in the slot jet configuration. This is illustrated in Fig. 8 where $\overline{Nu}/\overline{Nu}_\infty$ is plotted as a function of z/w for the contoured orifice

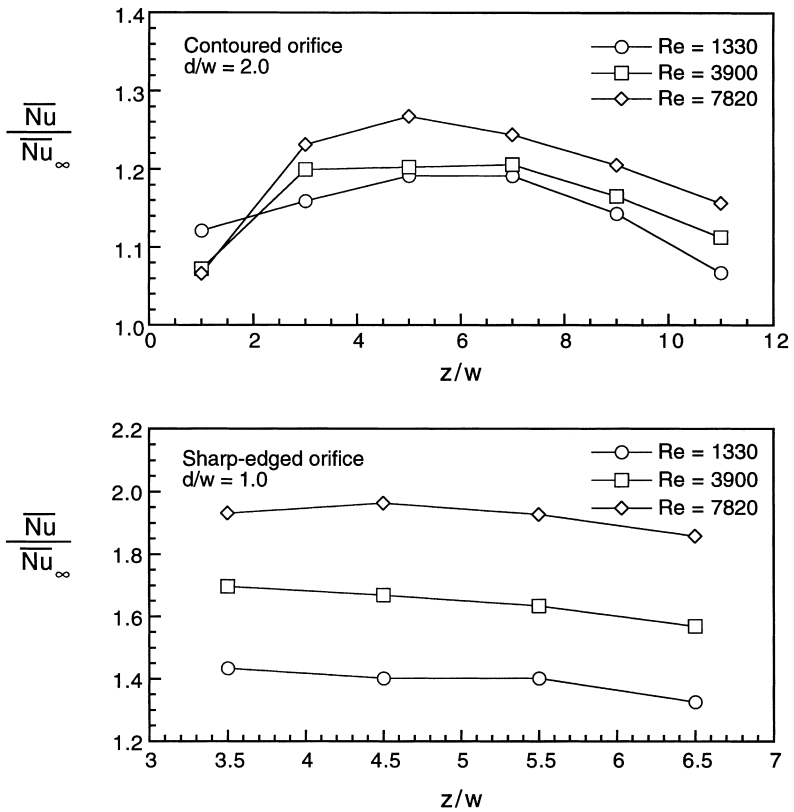

Fig. 8. Variation of $\overline{Nu}/\overline{Nu}_\infty$ with z/w for the contoured and sharp-edged orifices.

(d/w = 2.0) and sharp-edged orifice (d/w = 1.0) at the same three Reynolds numbers. The maximum in $\overline{Nu}/\overline{Nu}_\infty$ is clearly evident for the contoured orifice, with a peak in the enhancement of about 25% near z/w = 5. This is in agreement with previous studies at higher Re, where a maximum in average Nusselt number was observed for contoured orifices at $z/w \approx 6$–7 [5,6]. For the sharp-edged orifice the maximum in $\overline{Nu}/\overline{Nu}_\infty$ appears to occur at lower z/w, and is less pronounced (i.e., $\overline{Nu}/\overline{Nu}_\infty$ is less dependent on z/w). Data for the sharp-edged orifice at $z/w > 3.5$ for Re = 1330 and 3900 have presumably reached a peak and are now decreasing with increasing z/w. The peak in enhancement ratio at lower z/w for the sharp-edged orifice is perhaps due to the fact that the jet is effectively thinner for this configuration due to the vena contracta effect previously noted. Hence, the potential core is smaller, and it may be suggested that the *effective* jet width w is smaller for this nozzle than for the contoured orifice. Further, the turbulence level is possibly higher in the slot jet. A smaller effective nozzle width w for the sharp-edged orifice would have the effect of shifting the curves to higher z/w. No such maximum in the $\overline{Nu} \sim z/w$ relationship was observed in a previous study utilizing sharp-edged orifices [7]. It may generally be concluded that the thermally optimum spacing is 2–6 nozzle widths downstream of the jet exit, with the optimum for the contoured orifice occurring on the high side of this range ($z/w \approx 5$–6), and the optimum for the sharp-edged orifice occurring on the low side ($z/w \approx 2$–4).

The dependence of heat transfer enhancement ratio on nozzle width is shown in Fig. 9 for both orifice types studied at three Reynolds numbers. The nozzle-to-cylinder physical spacing for these data is constant at $z = 5\ d$. For the same physical location of the cylinder, increasing the jet width produces a maximum in Nusselt number. Although the maximum in $\overline{Nu}/\overline{Nu}_\infty$ is not reached for the sharp-edged orifice with decreasing d/w (due to limitations in the blower capacity), the heat transfer enhancement ratio should approach unity for $d/w \to 0$, since this asymptote corresponds to infinite parallel flow. The contoured orifice experiences the peak in heat transfer coefficient at higher d/w than the sharp-edged orifice. As suggested previously, the vena contracta associated with the sharp-edged orifice may result in a potential core more characteristic of a contoured orifice of smaller width w, with an associated shift in the $\overline{Nu}/\overline{Nu}_\infty$ curve in Fig. 9 to lower nozzle-widths.

The qualitative heat transfer dependence on geometric parameters governing the problem may be summarized graphically in Fig. 10. Fig. 10(a) illustrates the case where a given cylinder is located at different positions relative to the jet exit along the jet centerline for the same d/w. A position near the jet exit is characterized primarily by low-turbulence potential core flow washing the forward surface of the cylinder. In this case flow separation may also result, with poor flow coverage on the backside of the cylinder. The result is relatively lower heat transfer. When the cylinder is located near the tip of the potential core the flow's approach velocity is still relatively unaffected by the stagnant ambient fluid, and the high turbulence gener-

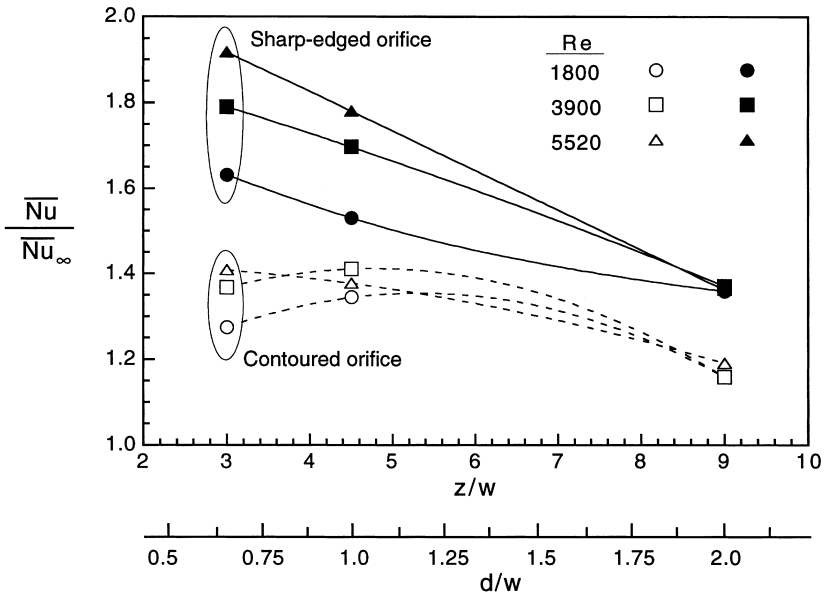

Fig. 9. Variation of $\overline{Nu}/\overline{Nu}_\infty$ with z/w (and corresponding d/w) for the two orifices studied.

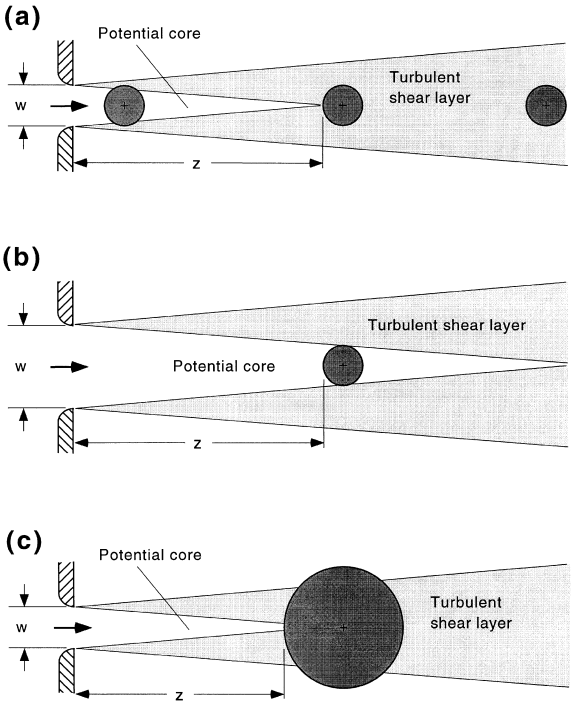

Fig. 10. Qualitative description of the free jet flow structure for various geometric combinations.

ated in the shear layer at the boundaries of the potential core cools much of the heated cylinder. The flow remains attached around much of the backside of the cylinder due to high momentum and turbulent energy. This condition corresponds to the optimum heat transfer seen by the peak in $\overline{Nu}$ (or $\overline{Nu}/\overline{Nu}_\infty$) observed in Figs. 7–9. The data presented previously indicates that this location is $z/w < 5$–6 for the contoured orifice, and $z/w < 4$ for the sharp-edged orifice. When the cylinder is positioned downstream of the potential core the fluid velocity is degraded from its nozzle exit value, and the cylinder is cooled ineffectively.

If the cylinder is placed at the end of the potential core for a given nozzle width, and the nozzle width is then doubled [as shown by the comparison of Fig. 10(a) and (b)], the cylinder's position relative to the potential core moves from the thermally optimum position upstream, where it is more fully engulfed by the lower-turbulence potential flow. If instead, the nozzle width were decreased (not shown), the cylinder would then lie downstream of the tip of the potential core. In either case the heat transfer is reduced from the maximum.

Fig. 10(c) illustrates what is speculated to happen if the diameter of the cylinder located at the optimum z/w is increased. As the cylinder size is increased, a portion of the cylinder may lie outside the turbulent shear layer, and turbulence may be suppressed by the favorable pressure gradient in the boundary layer developing along the cylinder's impingement surface. Indeed, for very large cylinders the flow may stagnate at the cylinder's forward stagnation point and never reach the backside of the cylinder. In this scenario the average heat transfer coefficient is likely to be reduced as d increases. The cylinder location normalized by the jet width z/w determines the cylinder's position relative to the jet potential core. The additional parameter which characterizes the cylinder diameter relative to the nozzle width d/w describes the nature of the cylinder's interaction with the jet potential core and turbulent shear layer.

The average Nusselt number data were correlated for the various experimental conditions with the functional form

$$\overline{Nu} = ARe^m \tag{4}$$

where the constants A and m were determined from a least-squares correlation of the data. The average and maximum error in the correlation for all data were 3.2% and 9.2%, respectively, in the range of Reynolds number studied here, $600 < Re < 8000$. The correlation constants are shown in Table 1 for both the con-

Table 1
Constants for the empirical correlation of Eq. (4)

z/w	$d/w = 2.0$		z/w	$d/w = 1.0$		z/w	$d/w = 0.66$		z/w	$d/w = 1.0$	
	A	m		A	m		A	m		A	m
Contoured orifice									*Sharp-edged orifice*		
1.0	0.65	0.48	0.5	0.49	0.54	0.33	0.62	0.51	3.5	0.22	0.67
3.0	0.44	0.54	1.5	0.49	0.54	1.0	0.60	0.51	4.5	0.20	0.68
5.0	0.33	0.58	2.5	0.45	0.55	1.66	0.53	0.53	5.5	0.19	0.68
7.0	0.30	0.59	3.5	0.41	0.56	2.33	0.57	0.52	6.5	0.17	0.69
9.0	0.28	0.59	4.5	0.41	0.56	3.0	0.54	0.53			
11.0	0.28	0.59	5.5	0.37	0.58	3.66	0.53	0.54			

toured and sharp-edged orifices. The correlations confirm that the sharp-edged orifice yields higher heat transfer coefficient than the contoured orifice. Generally, the Reynolds number dependence for the contoured orifice approaches $m = 0.5$ for decreasing d/w as is typical of infinite stagnation flow (which would prevail for $w \to \infty$). The observed dependence on Reynolds number is lower than what has been previously reported for contoured orifices at significantly higher Re with exponents m below 0.59, compared to $m = 0.6$–0.68 found previously [6]. Table 1 also shows that the average Nusselt number for the sharp-edged orifice exhibits markedly higher dependence on Reynolds number than the contoured orifice, as was seen in Fig. 6. Typical exponents are seen to be near $m \approx 0.7$ for this orifice, which is in agreement with higher-Re data reported previously [7].

4. Conclusions

The heat transfer characteristics of circular cylinders exposed to slot jet impingement of air has been studied experimentally for the Reynolds number (based on cylinder diameter) in the range 600–8000. Both contoured orifice and sharp-edged orifice jet configurations were investigated for values of the cylinder-to-nozzle width ratio $d/w = 0.66$, 1.0 and 2.0, and for a range of jet exit-to-nozzle width $z/w = 1$–11. Reference measurements were made with the same cylinder in infinite parallel flow in a wind tunnel. The results reveal that the slot jet yields considerably higher average heat transfer from the cylinder when compared to the infinite parallel flow case on the basis of identical slot jet and infinite flow average velocity. A dimensionless cylinder spacing z/w exists which exhibits a maximum in cylinder heat transfer. The optimum spacing is closer to the nozzle exit for the sharp-edged orifice than for the contoured orifice. The average Nusselt number shows stronger Reynolds number dependence for the sharp-edged orifice than for the contoured orifice.

References

[1] H. Martin, Heat and mass transfer between impinging gas jets and solid surfaces, Advances in Heat Transfer 13 (1977) 1–60.
[2] S.J. Downs, E.H. James, Jet impingement heat transfer — a literature survey, ASME paper 87-HT-35, ASME, New York, 1987.
[3] J.N.B. Livingood, P. Hrycak, Impingement heat transfer from turbulent air jets to flat plates — a literature survey, NASA TM x-2778, 1973.
[4] R. Viskanta, Heat transfer to impinging isothermal gas and flame jets, Exp. Therm. Fluid Sci. 6 (1993) 111–134.
[5] H. Schuh, B. Persson, Heat transfer on circular cylinders exposed to free-jet flow, Int. J. Heat Mass Transfer 7 (1964) 1257–1271.
[6] H. Kumada, I. Mabuchi, Y. Kawashima, Mass transfer on a cylinder in the potential core region of a two-dimensional jet, Heat Transfer — Japanese Research 2 (1973) 53–66.
[7] E.M. Sparrow, A. Alhomoud, Impingement heat transfer at a circular cylinder due to an offset or non-offset slot jet, Int. J. Heat Mass Transfer 27 (1984) 2297–2306.
[8] S.W. Churchill, M. Bernstein, A correlating equation for forced convection from gases and liquids to a circular cylinder in crossflow, ASME J. Heat Transfer 99 (1977) 300–306.
[9] T.G. Beckwith, N.L. Buck, R.D. Marangoni, Mechanical Measurements, 3rd ed., Addison-Wesley, Reading, MA, 1982.
[10] N.T. Obot, A.S. Majumdar, W.J.M. Douglas, The effect of nozzle geometry on impingement heat transfer under a round turbulent jet, ASME Paper 79-WA/HT-53, 1979.